Journal of Food Engineering 389 (2025) 112386

Contents lists available at ScienceDirect

Journal of Food Engineering

journal homepage: www.elsevier.com/locate/jfoodeng

The effect of surface chemistry on the caking behaviour of sucrose crystals

Amin Farshchi [a,*], Meishan Guo [b], Jabbar Gardy [c,d], Xun Zhang [e], Ali Hassanpour [c], Majid Naderi [b]

[a] School of Health and Life Sciences, Teesside University, TS1 3BX, UK
[b] Surface Measurement Systems, London, HA0 4PE, UK
[c] School of Chemical and Process Engineering University of Leeds, LS2 9JT, UK
[d] Cormica Bradford Limited, Listerhills Science Park, Campus Road, Bradford, BD7 1HR, UK
[e] School of Mechanical, Aerospace and Civil Engineering, University of Manchester, M13 9PL, UK

ARTICLE INFO

Keywords:
Caking
Sucrose
Food powder
Crystals
Moisture sorption

ABSTRACT

The caking behaviour of organic crystals presents a significant challenge in both the food and pharmaceutical industries. This study aimed to investigate how surface impurities influence the caking behaviour of sucrose (sugar) crystals. Sucrose crystals were selected as the model material due to their relevance in various industries such as food processing and pharmaceuticals. The impact of surface chemistry was assessed for sucrose crystals with varying levels of impurities, namely white sugar, light brown sugar, and dark brown sugar. These crystals were subjected to controlled cycles of humidity exposure, compaction, and drying to induce caking, simulating real-world scenarios. The caking propensity was evaluated using a compression test, while the surface chemistry was characterized through Inverse Gas Chromatography (IGC). Moisture sorption properties were evaluated using a Dynamic Vapor Sorption (DVS) technique, and the formation of solid bridges was studied using scanning electron microscopy (SEM) and X-ray computed tomography (XCT). The results indicate that impurities play a crucial role in enhancing the caking behaviour of sucrose crystals by influencing their hygroscopicity and facilitating solid bridge formation. This study provides valuable insights into the relationship between surface chemistry, moisture sorption properties, and the caking behaviour of sucrose crystals, offering strategies to mitigate caking issues.

1. Introduction

Sucrose, a widely recognized and commonly used sugar (α-D-glucopyranosyl β-D-fructofuranoside), exhibits unique properties that make it a versatile ingredient in the food and pharmaceutical industries. Sucrose crystals are typically processed and refined to be used in a wide range of applications. White sucrose that has undergone a refining process to remove impurities, can serve as a pharmaceutical excipient due to its desirable properties, including its ability to act as a bulking agent in tablets and a sweetening agent in various oral liquid medications, syrups, and suspensions to improve taste and enhance patient acceptability (Balbani et al., 2006). In food formulations, sucrose crystals, available in a range of colours such as dark brown sugar, light brown sugar or white sugar, as well as different sizes including crystalline or powdered forms, e.g., icing sugar, serve as multifunctional components (Goldfein and Slavin, 2015; Santos et al., 2018). They are used as a flavour enhancer, sweetener, texturizer, and bulking agent, providing desirable sensory attributes and functional properties to a wide range of products from baked goods and confectionery to beverages and frozen foods (Cotton et al., 1955). The specific shade of brown is determined by the amount of molasses on the surface of sucrose crystals. Molasses, a by-product of sugar refining process, is a residual syrup from the final stage of crystallization, at which stage further separation of sucrose from impurities (nonsucrose compounds) is not possible with conventional equipment. Invert sugar, ash, organic compounds, colouring materials, e.g., melanoidins, and moisture are the main impurities in brown sugar (Asadi, 2006).

In sugar processing, certain impurities, including raffinose, betaine and most amino acids do not react with lime during the refining process and remain in the juice throughout the subsequent processes, such as evaporation and centrifugation, and end up in molasses (Farshchi and Elahi, 2013; Kenter and Hoffmann, 2009). Invert sugar, depending on the purification method, can either be completely decomposed, as seen in beet processing, or partially decomposed through the partial liming

* Corresponding author.
E-mail address: a.farshchi@tees.ac.uk (A. Farshchi).

https://doi.org/10.1016/j.jfoodeng.2024.112386
Received 2 July 2024; Received in revised form 29 October 2024; Accepted 4 November 2024
Available online 5 November 2024

process in cane factories. In cases of complete elimination, invert sugar is decomposed by lime during the main liming process, forming lactic acid and other carboxylic acids. In the partial liming process, as practiced by cane sugar refiners, the remaining invert sugar ends up in molasses. Most colouring substances formed by the Maillard reactions, including melanoidins, are initially eliminated during purification. However, due to the key role of high temperatures in their formation, they are regenerated during evaporation and crystallization, ultimately ending up in molasses (Asadi, 2006). Despite the major role of sugar in producing thousands of food products, one of the challenges encountered when working with sugar granules, especially unrefined varieties like brown sugar, is their tendency to form clumps, commonly referred to as caking (Cotton et al., 1955).

Powder caking is a common problem encountered in the food, chemical and pharmaceutical and fertiliser industries during handling and processing of powders. This refers to the undesirable phenomenon of particle agglomeration resulting in the transformation of a formerly free-flowing powder into a cohesive solid mass. The extent to which a bulk powder material undergoes caking can vary widely, ranging from large lumps that can be broken down when subjected to stress to a permanent fusion of particles that alters the original material's characteristics. Caking causes technological challenges during powder handling, including transportation and storage, and in the worst-case scenario can bring the manufacturing process to a complete stop (Fitzpatrick et al., 2010). Consequently, the presence of caked materials often requires the utilisation of a de-caking process to break up cake structures in powders. However, this process entails additional resource requirements including time, manpower, and equipment. Additionally, in some cases, the process of de-caking can result in the formation of particles with altered quality compared to the original ones (Chen et al., 2018). Therefore, an enhanced understanding of caking mechanisms is essential for the development of efficient strategies to prevent or mitigate caking issues in powder handling technologies. There are many different caking mechanisms described in the literature. However, the majority of studies tend to focus on the caking phenomenon in amorphous powders rather than crystals. The caking of amorphous powders is typically attributed to a process involving moisture- or temperature-induced glass transition, where the viscous flow of rubbery materials at contact points between particles plays a significant role in the formation of caking. When exposing crystals to a moist environment, the mechanism of caking differs significantly from that of amorphous powders. Crystal caking is typically facilitated by the formation of liquid bridges at contact points between crystalline particles. This phenomenon arises from capillary condensation which can be viewed as the onset of deliquescence. Deliquescence takes place when a crystalline solid adsorbs water vapor molecules and transforms into an aqueous saturated solution at a critical relative humidity threshold (Carpin et al., 2016). Subsequently, if water is evaporated due to changes in ambient conditions such as relative humidity and/or temperature, recrystallization of the solute occurs, resulting in the formation of solid bridges between the crystalline particles.

In general, the factors that influence caking can be classified into two broad categories: intrinsic and extrinsic. Extrinsic factors refer to environmental conditions, such as temperature, relative humidity, and pressure or stress during storage or powder processing, that can affect the physical and chemical properties of powders. Intrinsic factors, on the other hand, pertain to the powder's inherent characteristics, including particle size, mechanical properties, surface energetics and surface chemical composition, that influence its caking behaviour. In the context of crystal caking, the surface chemical composition and surface energetics of crystals play a critical role in their interactions with water vapor molecules and hygroscopicity (Carvajal and Staniforth, 2006; Chen et al., 2018).

Among crystalline food particles, sucrose crystals stand out as a prime example, where the surface chemical composition can be varied depending on the type of sucrose crystal, whether it is purified or not, resulting in varying levels of impurities. By studying sucrose crystals with varying level of impurities on the surface, a better insight into the relationship between surface composition, moisture sorption properties, and the development of caking can be achieved. Such knowledge facilitates the development of effective strategies to prevent or mitigate caking in various applications involving crystal-based materials.

Previous studies have extensively examined the impact of temperature and relative humidity on the caking behaviour of sucrose crystals. Johanson and Paul (1996) investigated the influence of temperature cycling on various soluble materials, including sucrose crystals. Rastikian and Capart (1998) conducted experimental and theoretical studies on the heat and mass transfer within sugar storage silos, considering factors such as water sorption isotherm and thermal conductivity. Billings et al. (2006) focused on the caking phenomenon resulting from capillary condensation in humid environments. However, to the best of our knowledge, no previous studies have explored the influence of the surface chemistry of sucrose crystals on their moisture sorption and caking properties.

The present work, therefore, aims to address this crucial gap and provide a better understanding of how the surface chemistry of sucrose crystals, influenced by impurities, affects their moisture sorption behaviour and propensity for caking. To achieve this, the caked structure of three distinct sucrose crystals with varying levels of impurities, namely white sugar, light brown sugar, and dark brown sugar, was investigated using a compression test. The surface chemistry of the crystals was examined through the application of Inverse Gas Chromatography (IGC) and Attenuated Total Reflectance Fourier Transform Infrared Spectroscopy (ATR-FTIR). The influence of impurities on the moisture sorption characteristics of the sucrose crystals were analysed using a Dynamic Vapor Sorption (DVS) technique. The study also involved investigating the formation of solid bridges between particles by employing scanning electron microscopy (SEM) and X-ray tomography techniques. Additionally, to further understand how varying humidity levels impact the flow behaviour and compressibility of the sucrose crystals, bulk compression tests were employed. These tests helped evaluate the compressibility and powder flow properties of the crystals, providing crucial data on how relative humidity influences the cohesion and handling characteristics of these sugar forms.

2. Materials

Granulated sugar crystals with varying impurity levels, namely white sugar, light brown sugar, and dark brown sugar, were purchased from a local supermarket in the UK. The content of sugar substances in white, light brown, and dark brown sugar granules was determined to be approximately 100%, 99.7% and 98.2% respectively, as measured by direct polarimetry (without inversion) as described in Section 3.1. For caking characterisation, ATR-FTIR analysis, and tapped bulk density measurements, the sugar crystals were conditioned by storing the samples in desiccators at specific relative humidity levels at 21 $\pm$ 1 °C for a duration of four days. Detailed information about the conditioning process can be found in the methodology sections. Lithium chloride, magnesium nitrate and sodium chloride used to control RH at 11%, 54% and 75% during storage were purchased from Sigma-Aldrich.

3. Methodologies

3.1. Apparent sucrose content measurements

The sucrose content in sugar samples was determined using direct polarimetry, which measures the rotation of plane-polarized light by optically active substances in a solution. Conducted without inversion, this method detects the presence of all optically active sugars such as raffinose and glucose in addition to sucrose. This could explain the slightly elevated sucrose content reported for white sugar in the Materials section, which was as high as 100%, even though the typical

sucrose content of refined white sugar is approximately 99.95% according to the literature. (Asadi, 2006).

Measurements were carried out with a Bellingham + Stanley ADP450 Polarimeter, equipped with temperature control and a calibrated quartz control plate, stabilised overnight prior to use. Sugar samples were weight to 10.000 g (±0.0005 g) and dissolved to 100 mL with water in volumetric flasks. The solutions were thoroughly mixed until all solids were dissolved, using a magnetic stirrer. The dark brown sugar sample was filtered due to its turbidity using Whatman filter paper, discarding the initial 5 mL. Optical rotations were measured at a controlled temperature of 20.0 °C in a specially calibrated 100 mL tube, with zero calibration checks conducted before each measurement session. The apparent sucrose content was calculated from these rotations using the specific rotation of the AnalaR sucrose standard, which is 66.81° at 20 °C. The calculation for sucrose content is based on the following equation (Asadi, 2006):

$$Apparent\ sucrose\ content = \frac{Observed\ rotation}{[\alpha]_{Sucrose} \times L} \tag{1}$$

Where [α] = 66.81 is the specific rotation of the standard analytical sucrose at 20 °C, and L is the path length of the sample cell.

3.2. Colour measurements

The presence of colouring impurities in sugar granules was assessed using a UV–Vis spectrophotometer. Colour measurements were performed according to the guidelines of the International Commission for Uniform Methods of Sugar Analysis (ICUMSA), which are universally adopted in the sugar industry. Prior to the measurements, sugar solutions were prepared with different concentrations: 50% w/v for white sugar and 5% w/v for unrefined sugar granules. The initial pH of each solution was assessed and adjusted to pH 7.0 using carefully measured volumes of 0.1 N HCl and 0.1 N NaOH. The solutions were then filtered through a 0.45 μm filter. Absorbance was measured at 420 nm, and colour was calculated using the following equation (Asadi, 2006):

$$Colour\ (ICUMSA) = \frac{10^6 \times A}{b \times DS \times d} \tag{2}$$

Where A is the absorbance of the solution, b is the cell length (mm), DS is the refractometric Dry Substances (°Brix) and d is the density of the solution (g.ml^{-1}). The unit of colour expression is the ICUMSA unit (IU), also known as ICUMSA-420 colour.

Additionally, colour parameters of the sugar granules were determined using a hand-held spectrocolorimeter (Lovibond® LC100, China) employing the CIE D65 illuminant and a 10° observation angle. The colour measurements were expressed in terms of L*, a*, b*, C* and h. The colour parameter L* represents lightness, ranging from 0 (darkest) to 100 (lightest). The parameter a* indicates red to green colour, and b* value represents blue to yellow colour. The hue value (h°) in colour measurement represents the type of colour perceived by the human eye. It is essentially an angle expressed in degrees, determining the colour's position in a 360° grid where 0°, 90°, 180°, and 270° represent bluish-red, yellow, green, and blue colour, respectively. The chroma (C*) represents the saturation or purity of the colour.

The following equations derive the hue angle (h°), chroma (C*), and total colour difference (ΔE) (Aghajanzadeh et al., 2023):

$$Hue\ angle\ (h^\circ) = \tan^{-1}\frac{b^*}{a^*} \tag{3}$$

$$C^* = \sqrt{(a^*)^2 + (b^*)^2} \tag{4}$$

$$\Delta E = \sqrt{(\Delta L^*)^2 + (\Delta a^*)^2 + (\Delta b^*)^2} \tag{5}$$

where ΔL*, Δa*, and Δb* are the differences in colour parameters between the sugar granules and a white standard plate.

The obtained colour parameters L*, a* and b* were also used to determine the Browning Index, which defines the brown colour purity, calculated as follows:

$$BI = \frac{100 \times (z - 0.31)}{0.17} \tag{6}$$

where

$$z = \frac{a^* + 1.75\,L^*}{5.645L^* + a^* - 3.012b^*} \tag{7}$$

3.3. Bulk compression test and caking characterisation

Bulk compression testing and cake strength measurements were conducted using a texture analyser (Brookfield CT3 Texture Analyzer, Middleboro, MA, USA) equipped with a 50.0 kg-load cell with a resolution of 5.0 g. To investigate the effect of moisture sorption on the flowability and caking properties of sucrose crystals, approximately 5 g (±0.001) of sieve cuts (400–500 μm) were conditioned in desiccators at two different relative humidity levels: 54% and 75% RH. Following a 4-day humidification process, the sucrose crystals were carefully poured into an acrylic cylindrical split die with a diameter of 25.6 mm. The crystals were gently tapped for a duration of 3 min, continuing until no further reduction in volume was observed. Subsequently, the crystals were compressed under a normal force of 25 kg. The extent of particle bed displacement that occurred during the compression was then used to investigate the influence of storage relative humidity on the flowability of the conditioned sucrose crystals.

After the compression test, the die was exposed to a lower relative humidity (11% RH) for a duration of 4 days. The caked crystals were then removed, and their tensile strength was determined using the texture analyser. The uniaxial tensile strength was determined through the diametral-compression test, applying a constant speed of 0.1 mm/s. For this purpose, the tablets were placed on their sides and crushed along their vertical axis. The force-displacement curves obtained from the compression tests were subsequently analysed to calculate the tablet tensile strength, σ_t, as described by Fell and Newton (1970).

$$\sigma_t = \frac{F_r}{\pi r y} \tag{8}$$

Where F_r is the rupture force and r is the tablet radius, and y is the tablet thickness. The rupture force can be determined manually from the peak failure force in force-displacement curves, where the first sharp decrease in loading force can be observed (Fig. 1).

3.4. Hausner ratio and Carr's index

Tapped density measurements were used to characterise the flow behaviour of the sucrose granules. Hausner found that the ratio of tapped density to loose bulk density was related to interparticle friction. For loose bulk density measurements, a predetermined weight of the sucrose crystals conditioned at various relative humidity levels (54 and 75% RH) was gently poured into a 50.0 ml measuring cylinder, through a funnel positioned at a certain height. To determine the tapped density, the measuring cylinders were manually tapped on a flat surface for 60 s, continuing until no further change in crystal volume was observed. The flowability of sucrose granules was assessed using the Hausner ratio (HR), defined as the ratio of the tapped bulk density, ρ_{tapped}, to its initial bulk density, or loose bulk density, $\rho_{initial}$, which can be expressed as:

$$HR = \frac{\rho_{tapped}}{\rho_{initial}} \tag{9}$$

In general, a lower Hausner ratio of a powder signifies better flow characteristic (Hayes, 1987).

Carr's Index is a measure that quantifies the compressibility and

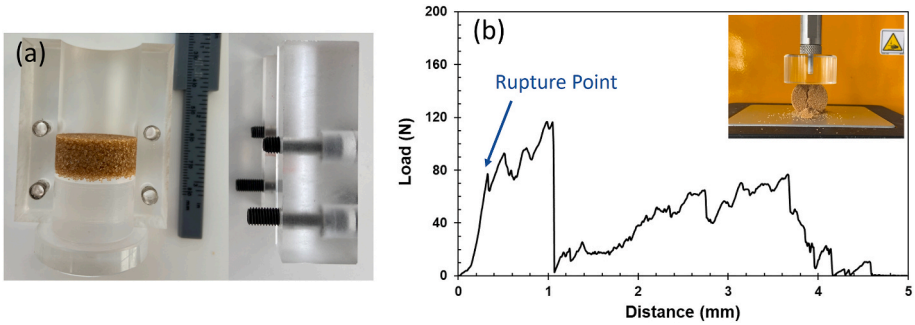

Fig. 1. Experimental setup and tablet compression behaviour. a) A split compaction die used for preparing caked sugar tablets. b) A Typical force-displacement curve obtained from the tablet compression test. Inset: Image capturing tablet fracture under compressive force.

flowability of a powder. A lower Carr's index indicates better flow characteristics. The Carr's Index is calculated using the following formula:

$$Carr's\ Index = \left(\frac{\rho_{tapped} - \rho_{initial}}{\rho_{tapped}}\right) \times 100 \quad (10)$$

3.5. Moisture sorption properties

The sorption behaviour of sucrose crystals was determined gravimetrically using a dynamic vapor sorption (DVS) technique (DVS Advantage, Surface Measurement Systems, Middlesex, UK). To ensure consistency and enhance the accuracy of the results, all sugar samples were sieved prior to the experiment. Approximately 100 mg of the sieved samples (400–500 μm) was placed in a sample pan, with an empty pan serving as a reference. The equilibrium moisture contents (EMC %) were obtained by incrementally increasing the humidity from 0% to 70% RH in 10% RH steps at a temperature of 25 °C. At each RH step, the sample was allowed to reach a gravimetric equilibrium, as indicated by a change in mass (dm/dt) lower than 0.002 % per minute, before progressing to the next RH step.

3.6. ATR-FTIR measurements

The presence of impurities, *i.e.*, molasses, and their moisture sorption properties within the granulated sucrose crystals were examined using Fourier Transform Infrared Spectroscopy (FTIR). Infrared spectra were acquired using a Nicolet iS10 FT-IR Spectrometer (Thermo Fisher Scientific, USA) employing the attenuated total reflection (ATR) method. The sucrose crystals were mounted on the top of a high-refractive index ATR crystal and then slightly pressed by a pre-mounted sample clamp. FTIR spectra were collected within the wavenumber range of 550–4000 cm^{-1} at a resolution of 4 cm^{-1}, with an average of 32 scans per sample.

3.7. Inverse gas chromatography (IGC)

The surface energy analysis was conducted using inverse gas chromatography with a Surface Energy Analyzer (IGC-SEA, Surface Measurement Systems Ltd., United Kingdom). Approximately 1.0 g of each sample was packed into individual silanized glass columns (300 mm length × 4 mm ID), and each end of the column was sealed with silanized glass wool to prevent sample movement during the experiment. Prior to the measurements, the columns were pre-conditioned for 2 h at 30 °C and 0% RH using nitrogen as the carrier gas to remove any physisorbed water. All experiments were performed at 30 °C with a total flow rate of 10 sccm (standard cubic centimetres per minute) of nitrogen, and methane was used for dead volume corrections.

The total surface energy (γ_s^t) is often considered to have two components: dispersive surface energy (γ_s^d) which represents the surface energy due to non-polar van der Waals interactions occurring at the surface and specific components (γ_s^{AB}) related to acid-base and polar interactions, e.g., hydrogen bonds and ionic bonds. The dispersive surface energy (γ_s^d) analysis was conducted by measuring the retention volume for a series of alkane eluants (heptane, octane, and nonane; HPLC grade, Sigma-Aldrich) using the Dorris and Grey method. The specific surface energy (γ_s^{AB}) was determined by measuring the retention volume of polar probe molecules (ethyl acetate and dichloromethane) on the samples using the Della Volpe scale (Ali et al., 2013). These energy components were presented as a function of surface coverage, expressed as the ratio n/n_m, where n is the number of moles of probe molecules injected and n_m is the monolayer capacity (Ho and Heng, 2013; Ho et al., 2012). These data sets were then modelled using a power function in Excel, chosen for its ability to represent the non-linear decrease in surface energy with increasing coverage effectively.

A description of the equations used in determining the surface energy through IGC measurements can be found in Voelkel's review (Voelkel et al., 2009). The experiments were performed to obtain average values with an R^2 coefficient better than 0.999 and the repeated identical runs of probe injections on each sample column showed that the standard deviation of the surface energy values is less than 3% at any given surface coverage.

The polarity of the samples was evaluated based on the relationship between the ratio of specific component of surface energy to the total surface energy $(\gamma_s^{AB}/\gamma_s^t)$. A higher polarity indicates a more hydrophilic nature or better wettability behaviour of the sample (Gamble et al., 2012).

3.8. Microscopic observation

The tendency of sucrose crystals to form cake structures, through the formation of solid bridges, was examined using scanning electron microscopy (SEM). To prepare the samples for SEM observations, sucrose crystals with a size range of 400–500 μm were affixed onto a double-sided adhesive pad mounted on a specimen stub. The SEM stubs were then placed in a desiccator with a relative humidity of 75% for four days, followed by transfer to another desiccator with a relative humidity of 11% for an additional four days. This conditioning process allowed for controlled exposure of the samples to different relative humidity conditions, facilitating the formation solid bridges between the sucrose crystals through the dissolution-recrystallization process.

3.9. X-ray micro-computed tomography

X-ray computed tomography is a non-destructive imaging technique capable of revealing internal structures of materials with micron to nano-scale resolution, making it suitable for studying the microstructure of caked granules. The internal structure of the caked sugar granules was analysed, both quantitatively and qualitatively, through the 3D reconstructed images obtained using an X-ray micro-computed tomography device (Zeiss Versa 520 XRM).

Following cycles of humidification, compression, and dehydration, the caked granules (or tablets) were carefully removed from the compaction split die and securely mounted on a rotating stage positioned between an X-ray source and detector. During the XCT data acquisition, the X-ray source operated at 80 kV, generating polychromatic X-rays. A lead-glass filter was used to achieve an optimal transmission rate. 1001 projections were collected as the samples were rotated by 360° incrementally with an exposure time of 3 s per projection. Three-dimensional volumes were reconstructed using the Scout-and-Scan™ Reconstructor software. The reconstructed virtual volume has a voxel size of 8.4 × 8.4 × 8.4 μm^3. These volumes covered a cylindrical field of view with dimensions of 8 mm in diameter and 8 mm in height. Fig. 2 shows a 2D XCT virtual slice illustrating the circular field of view this cylinder. The original volume was cropped, and a cube was created for further analysis. Subsequent analysis of the reconstructed 3D volumes was conducted using Avizo 2021 software.

A grey value threshold was initially applied to the grayscale histogram of the input virtual volume. A watershed segmentation algorithm was then employed to accurately segment the interparticle bridges within the caked sugar granules. The segmented regions underwent quantitative analysis to measure surface areas, providing insights into the caking behaviour of the granules. The extent of interparticle bridge formation was further analysed by calculating the specific surface area of the interparticle bridges. This was achieved by dividing the surface area of the segmented interparticle bridges by the total surface area of the sugar granules within the scanned region, thereby normalizing the bridge surface area relative to the overall granule surface area. The percentage of interparticle bridge formation was then calculated using the following formula:

$$\text{Percentage of bridge formation} = \frac{\text{Surface area of interparticle bridges}}{\text{Total surface area of sugar granules}} \times 100 \quad (11)$$

4. Results and discussions

4.1. Colour measurements

Colour is the first characteristic of sugar that attracts consumer attention. It is commonly accepted that the colour of sugar darkens as the purity decreases, with increases in impurities (Asadi, 2006). In Table 1 it can be seen that the L* values, representing lightness, decrease significantly from white to dark brown sugar. Specifically, dark brown sugar, with an L* value of 32.15, shows the most significant presence of colour impurities. The ΔE and BI values further illustrate the significant variation in appearance among different sugar types. The Browning Index, specifically, increases from 5.03 in white sugar to 30.97 in dark brown sugar, correlating with a decrease in lightness and an increase in perceived colour difference.

While spectrocolourimetry effectively compares the visual appearance of sugar granules, UV spectrophotometry links the level of colour to the chemistry of the impurities. This technique also mitigates the impact of crystal size, which can influence reflectance—a critical factor in colour measurement by spectrocolourimetry.

It has been reported that absorbance at 420 nm is associated with high molecular weight Maillard products (Patrignani and González-Forte, 2021), such as melanoidins, which are significant in colour formation during sugar processing. These melanoidins contribute to the darker colour observed in the UV spectrophotometry results, where ICUMSA-420 Colour units show a remarkable increase from 16.65 in white sugar to 10526.27 in dark brown sugar.

Additionally, when comparing the observed ICUMSA-420 Colour units with established industry standards (Asadi, 2006), the data for white and dark brown sugars align well within the expected ranges of 10–50 IU and 8500–11000 IU, respectively. However, the colour value for light brown sugar, typically between 2500 and 4000 IU, is noticeably lower, indicating slight variations that may be attributable to specific manufacturing processes.

4.2. Influence of relative humidity on the compression and caking behaviour of sucrose crystals

The compaction behaviour of the conditioned sugar crystals provides valuable insights into the impact of moisture sorption on their flowability and compressibility. This is notably evident when observing the bed displacement curves during incremental compression testing.

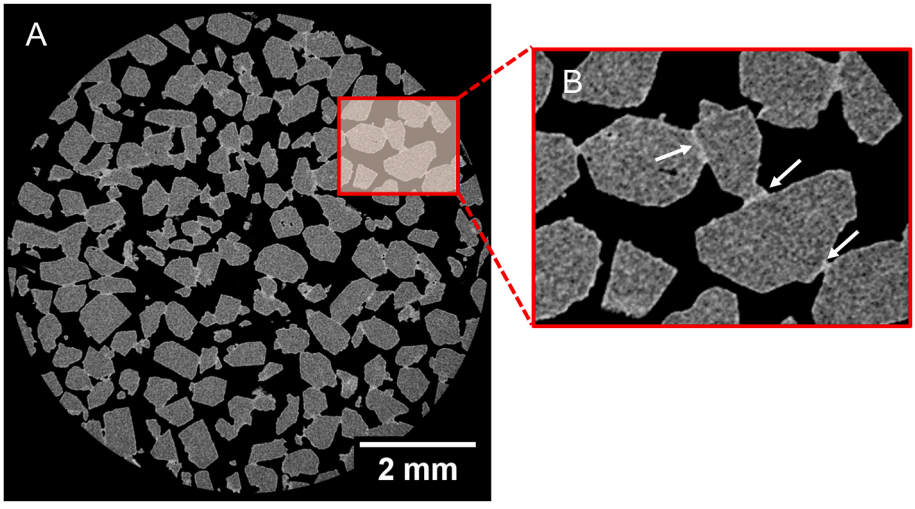

Fig. 2. A 2D filtered grayscale XCT virtual slice showing a circular field of view of the cylindrical volume. Inset: The arrows highlight the presence of interparticle bridges formed after cycles of humidification and dehydration, which will undergo further analysis using a watershed segmentation algorithm.

Table 1
Colour parameters and ICUMSA-420 colour values for different sugar granule types.

Sugar type	Colour parameters (Lovibond® Spectrocolorimeter)							UV Spectrophotometry
	L	a	b	c*	h°	ΔE	BI	ICUMSA-420 Color (IU)
White	80.3 ± 0.00	5.1 ± 0.57	4.1 ± 0.28	6.5 ± 0.57	38.65 ± 0.92	20.75 ± 0.21	5.03 ± 0.53	16.65 ± 0.92
Light brown	61.3 ± 3.25	6.85 ± 1.34	19.2 ± 0.85	20.4 ± 1.27	70.45 ± 2.76	43.8 ± 2.26	11.02 ± 1.09	1747.52 ± 11.47
Dark brown	32.15 ± 1.49	11.5 ± 1.27	20.5 ± 2.12	23.5 ± 2.40	60.65 ± 0.21	71.8 ± 0.57	30.97 ± 1.89	10526.27 ± 744.26

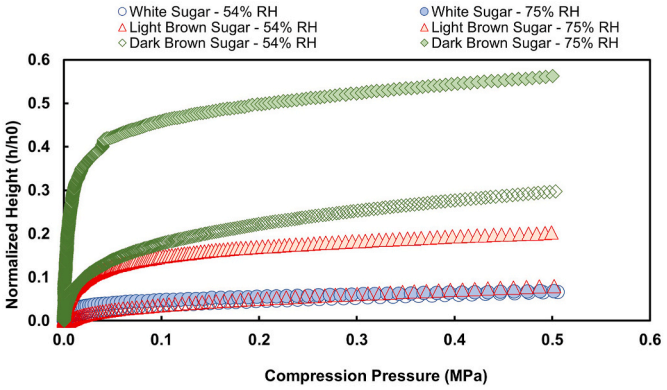

Fig. 3. Bed displacement of sugar granules under compression.

During compaction, the particles undergo deformation, rearranging and filling voids within the powder bed. As the bed deformation progresses through the rearrangement and sliding of particles, driven by the increasing normal stress, a reduction in bulk volume occurs due to the diminished interstitial spaces. For particles with good flow characteristics, the particle bed reaches a steady state at a lower compression pressure compared to more cohesive particles. This indicates a shorter displacement to reach the maximum force, even though the bed deformation may be prolonged.

Fig. 3 shows bed height during compression, normalized by the initial height, as a function of compression pressure. It is evident that the unrefined sucrose crystals displayed larger deformations within their respective particle beds when exposed to 75% RH. Notably, the influence of moisture sorption on compressibility was most pronounced in the case of dark brown sugar, where achieving a constant compression required the largest granule bed displacement. In other words, substantial deformation within the granule bed is necessary to attain a stable flow state. This can be attributed to their greater hygroscopicity, leading to a greater adhesion between wetted areas of the granules (Dopfer et al., 2013), and, consequently, the formation of more interstitial spaces within the bulk, which tend to collapse under increasing applied normal force.

Table 2
Physical properties of sugar granules at varied relative humidity: Hausner ratio, Carr's index, and tensile strength.

Sugar Type	HR		CI (%)		Tensile Strength (N/cm^2)	
	54% RH	75% RH	54% RH	75% RH	54% RH	75% RH
White Sugar	1.06 ± 0.01	1.03 ± 0.03	5.81 ± 1.13	4.36 ± 1.70	N/A	N/A
Light Brown Sugar	1.06 ± 0.01	1.15 ± 0.01	5.81 ± 1.13	13.2 ± 0.53	0.09 ± 0.02	2.79 ± 0.50
Dark Brown Sugar	1.07 ± 0.01	1.73 ± 0.03	6.74 ± 0.03	42.22 ± 0.89	8.86 ± 2.40	29.06 ± 7.10

Note: For white sugar granules, N/A (Not Applicable) as no caking was observed at the studied relative humidity values.

The results are in good agreement with the Carr's Index (CI) values obtained from bulk and tapped density measurements (Table 2), confirming the highest compressibility for dark brown crystals stored at 75% relative humidity (CI value of 42.22%). This corresponds to the earlier-discussed need for a relatively longer distance to achieve constant compression pressure in dark brown sugar crystals at 75% RH (Fig. 3). Interestingly, the Carr's Index and Hausner Ratio values obtained for white sugar stored at 75% relative humidity were found to be smaller than those for white sugar stored at 54% relative humidity, although these differences fall within the margin of error. One plausible explanation for this observation is that moisture may act as a lubricant at specific, low moisture contents, as potentially observed at 75% RH for white sugar in this study, thus improving the flow behaviour of particles (Stoklosa et al., 2012). However, at higher relative humidity levels, such as 85% RH, capillary adhering effects of water may become predominant, potentially leading to increased cohesivity.

The increased moisture-induced adhesion between the sugar granules, influenced by the presence of molasses impurities, was clearly manifested in the tablet strength measurements. White sugar granules, purified sucrose crystals, did not form integrated cake structures after cycles of humidification, compression, and dehydration. The resulting formed cakes were notably fragile and disintegrated immediately upon removal from the compaction die. In contrast, the brown sugar granules containing impurities, stored at both 54% and 75% RH, formed cohesive robust cakes. Both relative humidity level and surface impurities had a remarkable impact on tablet tensile strength. The tensile strength of tablets was remarkably higher for dark brown sugar granules at both relative humidity levels. This enhanced tensile strength can be attributed to the presence of higher levels of hydrophilic impurities of molasses compounds, including amides and reducing sugars, which consequently lower the critical deliquescence relative humidity of sucrose crystals, leading to the increased extent of interparticle liquid bridges during the humidification process.

The results for tablet strength can be better explained by both the 3D visualization and quantitative results obtained from the X-ray micro-CT technique, as well as by the microscopic observations. The increased bridge formation is evident in the 3D X-ray tomographs (Fig. 4), showing a higher level of interparticle bridge formation for the tablet of dark sugar granules stored at 75% RH. The interparticle bridge formation for dark brown sugar granules was 13.5%, while for light brown sugar granules it was 6.1%. The SEM images (Fig. 5) revealed that light brown sugar granules exhibited tiny solid bridges formed at points where crystals were in contact, while dark brown sugar granules showcased remarkable solid bridges between crystals. The altered morphology of dark brown sugar, characterised by the absence of sharp crystalline edges, suggests erosion or dissolution due to significant moisture sorption. These observations align with the higher tensile strength observed for the dark brown sugar granules, demonstrating a direct correlation between the extent of bridge formation and the resulting cake strength.

4.3. Surface energy

Surface energy, representing the excess of energy associated with a surface, was assessed to characterise the surface of sugar crystals. This energy arises from the unbalanced forces between the surface and the bulk. The total surface free energy is determined by both non-polar forces (dispersive) and polar forces (specific), and therefore, making it

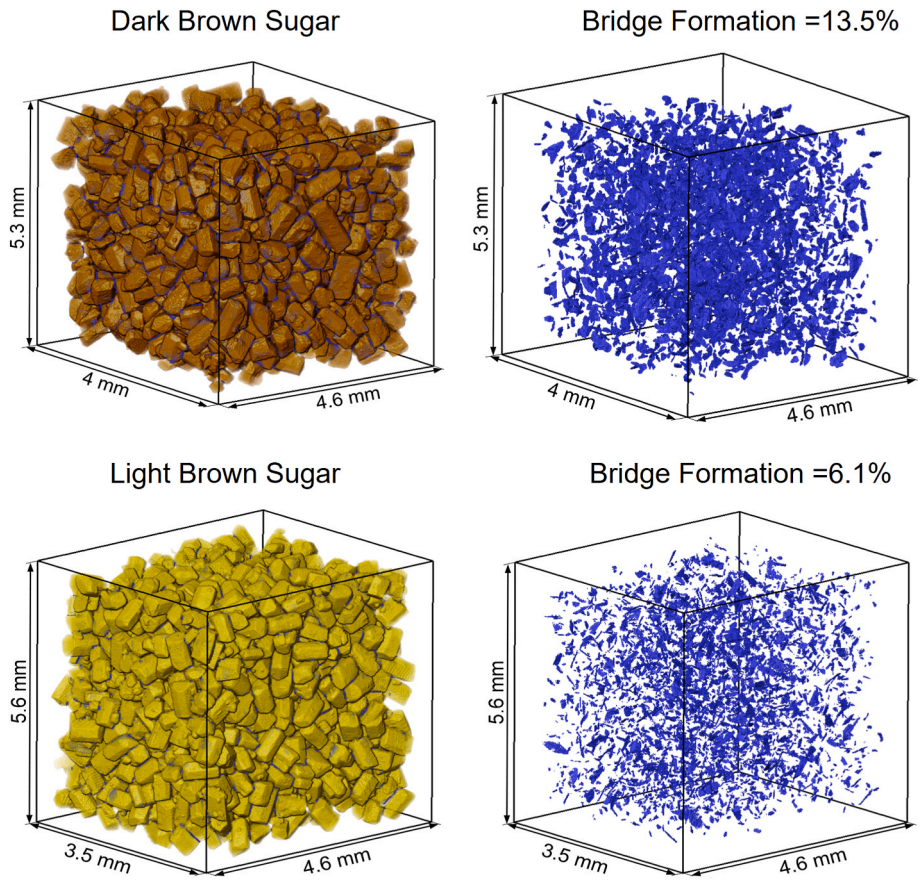

Fig. 4. 3D X-ray tomographs and corresponding segmented interparticle bridges of caked sugar granules. Left: 3D X-ray tomographs (voxel size: 8.4 × 8.4 × 8.4 μm^3) cropped from the original volume for the qualitative analysis of percentage of bridge formation for dark brown sugar granules (top) and light brown sugar granules (bottom). Right: Corresponding 3D volumes of the segmented interparticle bridges within the caked sugar granules, illustrating the interparticle bridges (blue) formed during the caking process.

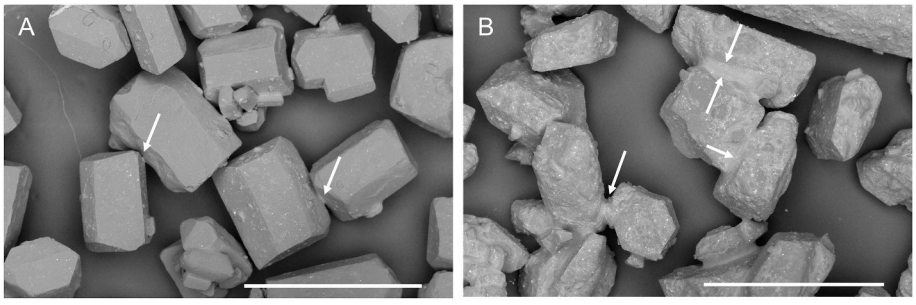

Fig. 5. Scanning Electron Microscopy (SEM) images of sugar granules exposed to 75% relative humidity (RH). Scale bars: A and B - 1 mm. A. Light brown sugar granules exhibiting tiny solid bridges (highlighted by arrows) formed at points where crystals were in contact. B. Dark brown granules showcasing remarkable solid bridges (highlighted by arrows) between crystals.

sensitive to the surface chemical composition (Martinez-Alejo et al., 2018). In the case of sucrose, the hydroxyl groups exposed on the surface contribute to the polar component, whereas the carbon atoms in the backbone affect the non-polar contribution.

Traditionally, surface energy measurements rely on contact angle measurements, a method suitable for flat homogeneous solids (Parsons et al., 1992). However, this study employed Inverse Gas Chromatography (IGC) to test surface energy, a technique proven effective for analyzing particles irrespective of their chemical nature, surface heterogeneity, area, and porosity (Martinez-Alejo et al., 2018).

Fig. 6 shows the dispersive, polar, and total surface energy as a function of surface coverage for different sugar granules. All the sugar granules showed a heterogeneous profile for dispersive and total surface energies, featuring high surface energy values that decreased with increasing surface coverage. Total surface energy values ranged from approximately 64.3 to 48.5 mJ/m^2 for white sugar, 63.0 to 47.7 mJ/m^2 for light brown sugar and 57.8–45.3 mJ/m^2 for dark brown sugar. Notably, the dispersive component significantly governed the total surface energy, with white sugar displaying the highest contribution, leading to a broader total surface energy distribution compared to unrefined sugar samples.

On the contrary, for all three tested samples, the polar component of the surface energy was negligible compared to the dispersive component. Additionally, no remarkable differences, within the margin of

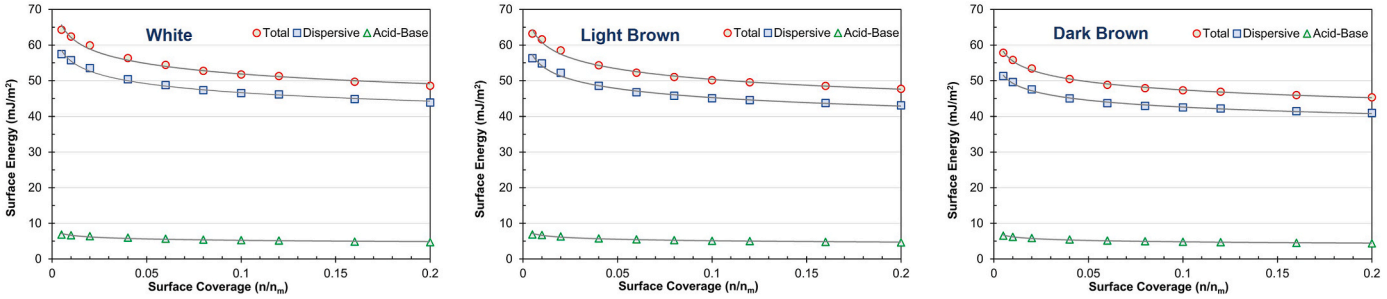

Fig. 6. Plots of total (γ_s^t), dispersive (γ_s^d), and acid-base (γ_s^{AB}) surface energies as a function of surface coverage for sugar granules. Surface coverage, denoted as n/n_m, represents the ratio of the quantity of adsorbed vapor molecules to the Brunauer-Emmett-Teller (BET) monolayer capacity for white, light brown, and dark brown sugar.

experimental errors, were observed in the measured specific surface energies. This suggests that molasses impurities did not play a dominant role in controlling the polar component of surface energetics. The specific surface energy values ranged from approximately 6.8 to 4.7 mJ/m^2 for white sugar, 6.9 to 4.7 mJ/m^2 for light brown sugar and 6.5–4.4 mJ/m^2 for dark brown sugar. This finding does not align well with the observed caking behaviour of brown sugar granules, which showed caking under humid conditions. It was expected that these granules would show higher specific surface energy because, in general, polar groups at the surface are typically responsible for enhancing wettability and, consequently, contributing to caking (Martinez-Alejo et al., 2018). A plausible explanation for the similarity in the measured specific surface energies is that the polar forces are predominantly influenced by the hydroxyl groups of sucrose exposed on the crystal surface rather than polar groups of non-sucrose compounds.

The ratio of the specific surface energy component to the total surface energy, known as surface polarity, has been previously associated with surface hydrophilicity (Ali et al., 2013). At low surface coverage, the probe molecules occupy the most hydrophilic sites, while the lower energy sites show greater hydrophobicity. Fig. 7 illustrates the degree of hydrophilicity for the sugar samples examined in this study. It can be seen that at low surface coverage, specifically below approximately 6%, the dark brown sugar sample shows a higher degree of hydrophilicity, indicating the prevalence of the most hydrophilic sites. This aligns with findings from Jange and Ambrose (2021), who investigated the impact of surface chemical composition changes due to molasses coating on the flowability of silica particles. Their study reported increases in both dispersive and specific surface energies, accompanied by a notable enhancement in surface basicity. This increase in basicity, driven by the molasses's rich electron donor components such as hydroxyl groups and amides, was correlated with increased cohesion, potentially influencing the material's flow properties. This is particularly relevant to this study, where the hydrophilic nature of sugar surfaces, especially those with higher molasses content, may lead to distinct interaction dynamics under humid conditions, as evidenced by the increased caking behaviour observed.

4.4. Moisture sorption properties

Water vapor sorption properties of the sugar granules were studied using DVS setup. Moisture sorption isotherms can provide valuable insights into how relative humidity affects the moisture content of sucrose crystals, and consequently influences their flowability and caking properties. The moisture sorption isotherms for sucrose crystals are shown in Fig. 8.

White sugar granules showed the lowest moisture uptake across all RH conditions among the samples tested. Given the particle size (400–500 μm) and temperature settings (25 °C) of the DVS measurements, the findings align with those of Billings and Paterson (2008) and Mathlouthi and Rogé, 2004. They reported a similar trend in equilibrium moisture content (EMC), specifically around 0.05 g/100g dry solids at 70% RH—the highest RH evaluated in this study. This behaviour is consistent with the observations of Samain et al. (2017) who reported minimal moisture uptake below 85% RH for purified sucrose crystals.

The unpurified sugar granules showed larger equilibrium moisture contents (EMC) across the entire RH range when compared with white sugar, suggesting a more hygroscopic characteristic. Overall, the dark brown sugar, showed the greatest affinity to absorb moisture from the surrounding air. The light brown sugar falls between white sugar and dark brown sugar in terms of sorption levels, indicating intermediate hygroscopic properties. All the samples showed a linear increase in moisture uptake for RH values up to 30%. However, exposure to higher relative humidity, particularly above 50% RH, resulted in a considerable

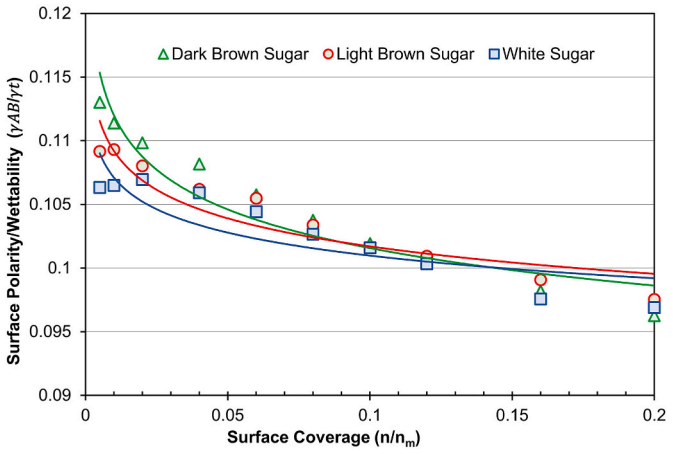

Fig. 7. Comparison of surface polarity/wettability $(\gamma_s^{AB}/\gamma_s^t)$ of different sugar granules as a function of fractional surface coverage.

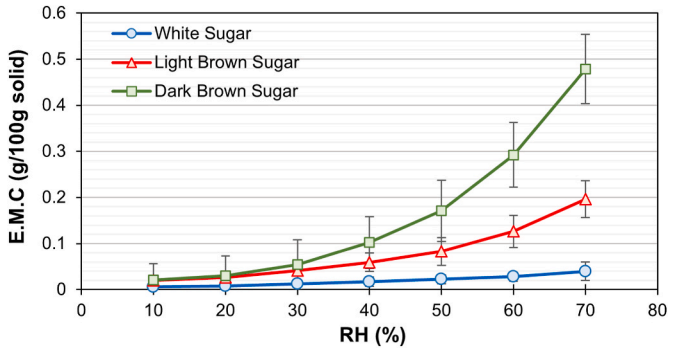

Fig. 8. DVS Equilibrium Moisture Content (EMC) for sugar granules as a function of relative humidity (RH).

change in moisture uptake for unpurified samples, with the effect being especially notable for dark brown sugar granules.

Research indicates that water vapor sorption at low relative humidity is primarily driven by entropy, which relates to the availability of sorption sites and the random movement of water molecules, dependent on the characteristics of the particle surface (Bonilla et al., 2010). In contrast, at medium to high relative humidity levels, moisture sorption involves interactions between the sorbate and sorbent, which may lead to structural alterations such as deliquescence, swelling, and glass transition. These changes facilitate the penetration of water molecules into the interior of the structures (Maher et al., 2014).

The noticeable increase in EMC values above 50% RH, signifies a shift in the mechanism of water sorption. For crystalline substances, at low relative humidity values, typically between 5% and 35% RH, sorption occurs with a few layers of water molecules at the surface of solids (Afrassiabian et al., 2016). With increasing the RH, the adsorbed layer becomes thicker, particularly in confined spaces such as contact points between particles or surface asperities at high relative humidity values leading to formation of liquid-like meniscus by capillary condensation. This may give rise to the partial dissolution of the crystal which consequently forms a saturated aqueous solution. When the ambient relative humidity reaches or exceeds a certain threshold value called Deliquescence Relative Humidity (DRH), the solid begins to deliquesce resulting in formation of a condensate film on the surface of the material. In the current DVS study, although the highest target relative humidity is well below the DRH of white sucrose (85%) at 25 °C, a sharp increase of moisture uptake for brown sugar above 50% RH, can be attributed to the onset of capillary condensation induced by the presence hygroscopic impurities.

The influence of molasses impurities on the moisture uptake capacity of the samples can be more thoroughly examined through ATR-FTIR studies conducted on the samples stored at different relative humidity levels. The evolution of FTIR spectra in relation to relative humidity is shown in Fig. 9. As displayed in this figure, for the samples exposed to a higher relative humidity (75% RH), the broad band in the 3000–3700 cm^{-1} region belonged to O-H stretching vibrations was observed to increase. This suggests a greater population of water molecules bound to the hydrophilic binding sites (Farshchi et al., 2019). The dark brown granules; however, showed the most significant increase in the intensity of bands in this region which can be attributed to water adsorption in the OH group of hygroscopic impurities such as invert sugars and raffinose, providing more active binding sites on the granule surfaces.

In the ATR-FTIR study, the presence of amide compounds as impurities and their moisture-induced spectral changes were clearly noticeable for dark brown sugar. At 54% RH, distinctive spectral features were observed with two broad peaks at ~1640 cm^{-1} and ~1560 cm^{-1}, corresponding to amide I and amide II bands, respectively. These absorption bands are assigned to symmetrical stretching vibrations of C=O functional groups, symmetrical bending vibrations of N-H groups, and symmetrical stretching vibrations of C-N groups (Patrignani et al., 2023). Such amide bands could be linked to the presence of amides such as glutamine, which exist as impurities in molasses. Glutamine, which constitutes about 50% of the amino acid content in beet juice, primarily decomposes into pyrrolydone-carboxylic acid (PCA) and, to a lesser extent, glutamic acid during purification. However, depending on the degree of purification, some glutamine remains in the juice throughout the process and ultimately appears as impurities on the surfaces of unrefined sugar granules (Farshchi and Elahi, 2013).

5. Conclusion

This study highlights the significant influence of surface chemistry on the caking behaviour of sucrose crystals. By examining sucrose crystals with varying levels of impurities, valuable insights into the relationship between surface composition, moisture sorption properties, and the development of caking were achieved. The granules were subjected to cycles of humidification, compaction, and drying to simulate real-world scenarios, revealing that surface impurities enhance their hygroscopicity, leading to increased caking propensity. The compression tests showed that dark brown sugar exhibits the highest tendency for caking. Surface energy analysis conducted through Inverse Gas Chromatography (IGC) confirms that the dispersive component predominantly governs the total surface energy, although detailed hydrophilicity analysis from IGC measurements revealed that the most hydrophilic sites are prevalent at low surface coverage in dark brown sugars. This observation was supported by moisture sorption studies using Dynamic Vapor Sorption (DVS) and Attenuated Total Reflectance Fourier Transform Infrared Spectroscopy (ATR-FTIR), which revealed a pronounced affinity for moisture in brown sugar samples, particularly dark brown sugar. Microscopic observations and X-ray computed tomography effectively elucidate the hygroscopic characteristics of unpurified sugars, highlighting the formation of interparticle solid bridges during cycles of humidification and dehydration.

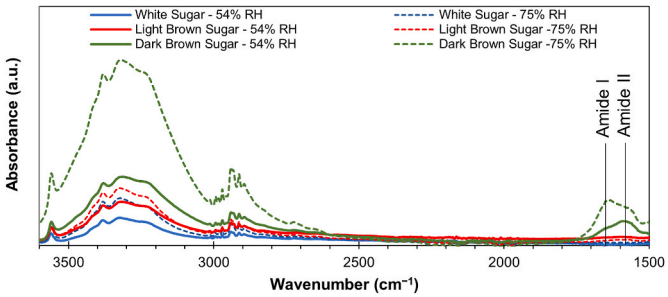

Fig. 9. ATR-FTIR Spectra (1500–3600 cm^{-1}) of sugar granules stored at 54% and 75% RH. Solid lines represent the spectra at 54% RH, while dashed lines indicate 75% RH.

The presence of hydrophilic molasses compounds on the surface of these granules enhances moisture uptake, leading to surface dissolution which, upon dehydration, solidifies to form robust solid bridges. These insights illuminate the complex interplay between surface chemistry and moisture dynamics in sugar granules, providing a foundation for developing strategies to mitigate caking and improve product handling and stability.

These findings offer practical implications for engineers, scientists, and product development professionals focused on enhancing product quality and stability. By understanding the role of impurities and surface chemistry in caking, strategic improvements can be made in the handling, processing, and storage of sucrose crystals and similar crystalline materials.

CRediT authorship contribution statement

Amin Farshchi: Writing – original draft, Methodology, Funding acquisition, Formal analysis, Data curation, Conceptualization. **Meishan Guo:** Methodology, Investigation. **Jabbar Gardy:** Investigation. **Xun Zhang:** Methodology, Investigation. **Ali Hassanpour:** Writing – review & editing. **Majid Naderi:** Methodology, Investigation.

Declaration of competing interest

The authors declare that they have no known competing financial interests or personal relationships that could have appeared to influence the work reported in this paper.

Acknowledgement

This work was supported by the National Research Facility for Lab X-ray CT (NXCT) through EPSRC grant EP/T02593X/1. We also acknowledge the contributions of David Parton-Ginno and John Wright

of Xylem Water Solutions UK Ltd. for their expert polarimetry analysis.

Data availability

Data will be made available on request.

References

Afrassiabian, Z., Leturia, M., Benali, M., Guessasma, M., Saleh, K., 2016. An overview of the role of capillary condensation in wet caking of powders. Chem. Eng. Res. Des. 110, 245–254.
Aghajanzadeh, S., Ziaiifar, A.M., Verkerk, R., 2023. Effect of thermal and non-thermal treatments on the color of citrus juice: a review. Food Rev. Int. 39, 3555–3577.
Ali, S.S.M., Heng, J.Y.Y., Nikolaev, A.A., Waters, K.E., 2013. Introducing inverse gas chromatography as a method of determining the surface heterogeneity of minerals for flotation. Powder Technol. 249, 373–377.
Asadi, M., 2006. Beet-sugar Handbook. John Wiley & Sons.
Balbani, A.P.S., Stelzer, L.B., Montovani, J.C., 2006. Pharmaceutical excipients and the information on drug labels. Brazilian Journal of Otorhinolaryngology 72, 400–406.
Billings, S.W., Bronlund, J.E., Paterson, A.H.J., 2006. Effects of capillary condensation on the caking of bulk sucrose. J. Food Eng. 77, 887–895.
Billings, S.W., Paterson, A.H.J., 2008. Prediction of the onset of caking in sucrose from temperature induced moisture movement. J. Food Eng. 88, 466–473.
Bonilla, E., Azuara, E., Beristain, C.I., Vernon-Carter, E.J., 2010. Predicting suitable storage conditions for spray-dried microcapsules formed with different biopolymer matrices. Food Hydrocolloids 24, 633–640.
Carpin, M., Bertelsen, H., Bech, J.K., Jeantet, R., Risbo, J., Schuck, P., 2016. Caking of lactose: a critical review. Trends Food Sci. Technol. 53, 1–12.
Carvajal, M.T., Staniforth, J.N., 2006. Interactions of water with the surfaces of crystal polymorphs. Int. J. Pharm. 307, 216–224.
Chen, M., Wu, S., Xu, S., Yu, B., Shilbayeh, M., Liu, Y., Zhu, X., Wang, J., Gong, J., 2018. Caking of crystals: characterization, mechanisms and prevention. Powder Technol. 337, 51–67.
Cotton, R.H., Rebers, P.A., Maudru, J.E., Rorabaugh, G.U.Y., 1955. The role of sugar in the food industry. In: Use of Sugars and Other Carbohydrates in the Food Industry. American Chemical Society.
Dopfer, D., Palzer, S., Heinrich, S., Fries, L., Antonyuk, S., Haider, C., Salman, A.D., 2013. Adhesion mechanisms between water soluble particles. Powder Technol. 238, 35–49.
Farshchi, A., Elahi, M., 2013. Influence of temperature and residence time of main liming process on the reduction of α-amino acids during beet juice purification. Int. Sugar J. 115, 108–114.
Farshchi, A., Hassanpour, A., Ettelaie, R., Bayly, A.E., 2019. Evolution of surface micro-structure and moisture sorption characteristics of spray-dried detergent powders. J. Colloid Interface Sci. 551, 283–296.
Fell, J.T., Newton, J.M., 1970. Determination of tablet strength by the diametral-compression test. J. Pharmaceut. Sci. 59, 688–691.
Fitzpatrick, J.J., Descamps, N., O'meara, K., Jones, C., Walsh, D., Spitere, M., 2010. Comparing the caking behaviours of skim milk powder, amorphous maltodextrin and crystalline common salt. Powder Technol. 204, 131–137.
Gamble, J.F., Leane, M., Olusanmi, D., Tobyn, M., Šupuk, E., Khoo, J., Naderi, M., 2012. Surface energy analysis as a tool to probe the surface energy characteristics of micronized materials—a comparison with inverse gas chromatography. Int. J. Pharm. 422, 238–244.
Goldfein, K.R., Slavin, J.L., 2015. Why sugar is added to food: food science 101. Compr. Rev. Food Sci. Food Saf. 14, 644–656.
Hayes, G.D., 1987. Food Engineering Data Handbook. Longman Scientific & Technical, Harlow.
Ho, R., Heng, J.Y.Y., 2013. A review of inverse gas chromatography and its development as a tool to characterize anisotropic surface properties of pharmaceutical solids. KONA Powder and Particle Journal 30, 164–180.
Ho, R., Naderi, M., Heng, J.Y.Y., Williams, D.R., Thielmann, F., Bouza, P., Keith, A.R., Thiele, G., Burnett, D.J., 2012. Effect of milling on particle shape and surface energy heterogeneity of needle-shaped crystals. Pharmaceut. Res. 29, 2806–2816.
Jange, C.G., Ambrose, R.P.K., 2021. Quantifying the influence of surface chemical composition on surface energy during powder flow. Part. Sci. Technol. 39, 192–203.
Johanson, J., Paul, B., 1996. Eliminating caking problems. Chem. Process 59, 71–75.
Kenter, C., Hoffmann, C.M., 2009. Changes in the processing quality of sugar beet (Beta vulgaris L.) during long-term storage under controlled conditions. Int. J. Food Sci. Technol. 44, 910–917.
Maher, P.G., Roos, Y.H., Fenelon, M.A., 2014. Physicochemical properties of spray dried nanoemulsions with varying final water and sugar contents. J. Food Eng. 126, 113–119.
Martinez-Alejo, J.M., Benavent-Gil, Y., Rosell, C.M., Carvajal, T., Martinez, M.M., 2018. Quantifying the surface properties of enzymatically-made porous starches by using a surface energy analyzer. Carbohydr. Polym. 200, 543–551.
Mathlouthi, M., Rogé, B., 2004. Caking of white sugar and how to prevent it. Proc S Afr Sug Technol Ass 495. Citeseer.
Parsons, G.E., Buckton, G., Chatham, S.M., 1992. The extent of the errors associated with contact angles obtained using liquid penetration experiments. Int. J. Pharm. 82, 145–150.
Patrignani, M., González-Forte, L.D.S., 2021. Characterisation of melanoidins derived from Brewers' spent grain: new insights into their structure and antioxidant activity. Int. J. Food Sci. Technol. 56, 384–391.
Patrignani, M., González-Forte, L.D.S., Rufián-Henares, J.Á., Conforti, P.A., 2023. Elucidating the structure of melanoidins derived from biscuits: a preliminary study. Food Chem. 419, 136082.
Rastikian, K., Capart, R., 1998. Mathematical model of sugar dehydration during storage in a laboratory silo. J. Food Eng. 35, 419–431.
Samain, S., Dupas-Langlet, M., Leturia, M., Benali, M., Saleh, K., 2017. Caking of sucrose: elucidation of the drying kinetics according to the relative humidity by considering external and internal mass transfer. J. Food Eng. 212, 298–308.
Santos, L.C.D., Condotta, R., Ferreira, M.D.C., 2018. Flow properties of coarse and fine sugar powders. J. Food Process. Eng. 41, e12648.
Stoklosa, A.M., Lipasek, R.A., Taylor, L.S., Mauer, L.J., 2012. Effects of storage conditions, formulation, and particle size on moisture sorption and flowability of powders: a study of deliquescent ingredient blends. Food Res. Int. 49, 783–791.
Voelkel, A., Strzemiecka, B., Adamska, K., Milczewska, K., 2009. Inverse gas chromatography as a source of physiochemical data. J. Chromatogr. A 1216, 1551–1566.